International Journal of Industrial Electronics, Control and Optimization © 2021 IECO
Vol. 4, No. 1, pp. 67-76, Jan (2021)

Dynamic Improvement of DC Microgrids with CPLs Using Virtual Inertia Concept

Mehran Jami[1, †], Qobad Shafiee[2], and Hassan Bevrani[3]

[1,2,3] Smart/Micro Grids Research Center, University of Kurdistan, Sanandaj, Iran

ABSTRACT

In this paper, a virtual inertia control strategy based on linear feedback is presented that improves dynamic behavior of islanded dc microgrids interfaced with constant power loads (CPLs). In order to solve the stability challenges caused by low inertia and CPLs, the proposed control scheme is composed of a virtual capacitor and a virtual conductance. It is implemented in the inner loop control, i.e. current loop control to be fast enough emulating inertia and damping concept. In addition, the droop characteristic is modeled by using the virtual resistance which adjusts the steady-state response of the system. In this study a multi-level structure is considered, which comprises the source level, interface converter level, and common load level. In addition, an accurate small-signal model is used to investigate the stability of dc MG interlaced with CPLs, and then, an acceptable range of inertia response parameters is determined by using the root locus analysis. Performance of the proposed control structure is demonstrated through numerical simulations.

Article Info

Keywords:

Constant power load, Dc microgrid, Dynamic response, Virtual capacitance, Virtual inertia.

Article History:

Received 2020-02-26

Accepted 2020-05-27

I. INTRODUCTION

Recently dc microgrids (MGs) have attracted more attention because of the increasing use of dc energy sources, energy storages, and loads in power systems. In these systems, challenges like reactive power flow, synchronization and power quality problems-which are challenge for ac systems, do not exist [1]. Fig. 1 shows a typical dc MG. Due to the probable and random nature of wind and solar resources, the bigger and more power imbalance is happened between the generation and consumption. This is a clear reason for reduction of MGs inertia in the presence of distributed generation sources [2]. Furthermore, if these resources are definite and constant, due to the lack of rotating energy and connection of these resources through the power electronic interface to the power system, the system inertia is reduced, which causes an increase in voltage fluctuations from the nominal value and decreases the security of the MGs. Obviously, the high amount of inertia increases the kinetic energy of the grid. This feature reduces the voltage fluctuations and increases the capability of the grid to compensate the energy imbalance that happened due to probable occurrences or load changes [3].

Several solutions are presented to increase the system inertia with high penetration of renewable energy in ac MGs [4]-[8]. Some of the control strategies are designed in such a way that power electronic converter emulates the synchronous machines behavior. The great advantage of power electronic converters is that the desired output power is generated by using proper control mechanism. These methods are based on simple derivative-proportional droop control rules [5]-[6] or more sophisticated control schemes which are called virtual synchronous generators (VSG) [7]-[9]. In VSGs, by using power electronic converter, fast-response energy storage and the special control mechanism, inertia for RESs is created. This strategy is also known as virtual inertia (VI). In some studies, VI is used to operate a grid connected inverter as a VSG [10], [11]. Droop control is well- known method to solve the low inertia issue by limiting the frequency and voltage changes within the permitted range. By comparison between

†**Corresponding Author**: m.jami@eng.uok.ac.ir
Tel: +98-9363949565, University of Kurdistan.
Department of Electrical and Computer Engineering, University of Kurdistan, Sanandaj, Iran

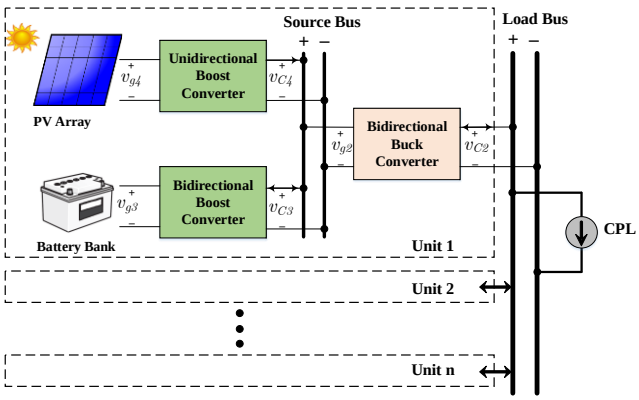


Fig. 1. Structure of a typical dc MG with CPL.

conventional droop control and VSG control, a generalized droop control is presented in [12]. In [13] and [14], a modified droop control method using fuzzy logic is designed based on the inertia injection, which injects adaptive virtual inertia instead of modeling the constant inertia. By selecting appropriate values of inertia and damping, proper performance of a VSG is guaranteed. In [15], a robust control method is used for fine-tuning the virtual parameters.

At present, researches on the VI control in dc MGs are hardly reported. The concept of VI control strategy is derived from the concept of VSG to regulate the dc bus voltage in a dc MG [16], [17]. In [16], a VI control strategy analogized with VSG is proposed to increase the inertia of the dc MG. However, integral feedback that used in this method not provides fast inertia in the first moment after disturbances. Furthermore, for droop-controlled converters in dc grids, the compromise between primary voltage regulation and damping coefficient needs to be considered. Increasing the inertia of photovoltaic (PV) systems through inertia emulation in autonomous MGs is presented in [18] and [19]. In these studies, for increasing inertia in a dc MG, VI control is generally employed in grid connected ac–dc type converters. In [20], adaptive VI control is proposed for the photovoltaic (PV) connected converter to eliminate the need of high-power storage for inertia emulation in a dc MG. However, utility of this method is limited by the availability of PV power and virtual damping coefficient has not been considered in the controller design procedure. In [21], the concept of a virtual dc machine is used to imitate the inertia specification of a dc machine in dc MGs through the control of the bidirectional dc–dc converters. The above mentioned VI control strategies, however, are inefficient in the presence of constant power loads (CPLs).

The research of CPLs in dc systems is essential to marine systems, automotive and aircraft applications [22]. From the source bus point of view, when a power electronic converter tightly regulates its output voltage with resistance load, it behaves like a CPL. The CPL has a positive instantaneous impedance but a negative incremental impedance. Hence, once the source bus voltage increases, the input current decreases and vice versa. This decreases the system's damping and makes the system more prone to oscillation [23]. Many solutions have been introduced for dc-dc power converters interfaced with CPL. One of the basic methods to overcome the CPL problem is by passive damping filters e.g., adding damping resistors in parallel or series with the inductor or capacitor of the filter [24]. Although this solution is simple and effective, it is costly and limited by physical constraints [22]. Another simpler and more effective way to tackle the CPL problem is using active damping. An active damping technique is implemented by control loops while emulating the passive elements. Due to the negative-impedance characteristics of CPLs and the nonlinearity of converters, nonlinear control strategies have been used to stabilize system, for instance, robust control [25], input-output linearization techniques [26], nonlinear control based on back stepping and nonlinear disturbance observer techniques [27]. Comparing with linear control methods, nonlinear ones are limited in practice because of a high requirement for the hardware configuration, more complication and extra cost [28]. In [29], the concept of smart resistor is proposed to dynamically stabilize CPLs at the point of load, wherein the equivalent load impedance can be made resistive instantaneously with energy storage units and high-bandwidth power converters. However, it is usually also not justifiable to install costly power conditioning modules only for stabilization purposes because they reduce the economic prospects and reliability of the whole system. In [30], a virtual resistance is created in series with the output of the converter. However, it leads to a significant drop in the output voltage at heavy loads resulting in poor voltage regulation. To overcome this drawback, the authors in [31] propose a virtual parallel resistive-inductive branch at the output of the source side converters feeding the CPLs. For improving the stability of the dc microgrid system, a virtual negative inductor [32] and virtual impedance [33] are constructed on the output of source-side converter. However, these methods suffer from some disadvantages:1) these methods only focus on solving the stability and voltage regulation problems while they are ineffective in improving the inertia response, and 2) when step changes or random fluctuations occur from the intermittent power resources and load power, low frequency oscillation appears, which results in lower dc voltage quality.

In this paper, the emulation of inertia and damping using derivative and proportional terms is proposed for islanded dc MGs with CPLs. This emulation is implemented in the inner current control loop. The fast and slow dynamics of the system have various effect on the voltage profile. The fast dynamics are directly related to the internal control loop i.e., voltage and current controllers. The slower transient dynamics are established by the virtual impedance control, droop mechanism and interactions between them. Therefore, by adding proportional and derivative signals of dc bus voltage to current controller with a particular mechanism, the rate of

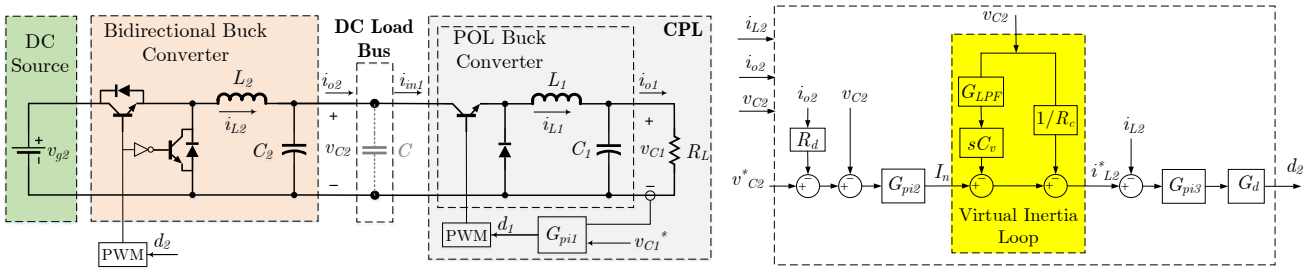


Fig. 2. Simplified structure of a typical dc MG with CPL: (a) detailed power conversion circuit, (b) proposed control diagram for a bidirectional buck converter.

injection inertia to the system will be increased. The salient features of this paper are as follows:

- The proposed virtual control strategy is based on a linear feedback. It uses measurement of the output voltage and current in source-side converter in order to guarantee the stable operation and to enhance the damping of dc MGs with CPLs. Opposed to the existing virtual-impedance-based stabilizations in [31], [32] and [33], which are focused only on the stability improvement, the proposed controller improves dynamic response with decreasing rate of change of voltage (RoCoV).
- The proposed derivative term in the inner control loop decreases rate of change of dc bus voltage by using virtual capacitance that emulates inertia concept. Comparing with the existing virtual inertia control in [16] and [17], which implements in droop control loop, the proposed virtual inertia provides faster inertia response to decrease the RoCoV in the first moment after disturbances due to the derivative feedback is implemented in inner current loop.
- The proposed proportional term in the inner current control increases damping of dc bus voltage by using virtual conductance that emulates damping coefficient concept. Opposed to the existing virtual damping coefficient in [16] and [17], which increases the negative impact on voltage regulation performance, the proposed proportional term in the virtual inertia loop does not affect the steady state voltage.
- The small-signal stability analysis is used to study the system behavior under small distortion or load deviation at the presence of the proposed control loop. The proposed method is evaluated using the eigenvalue analysis and time-domain simulations.

The rest of this paper is divided into five sections. In Section II, the proposed control strategy is introduced based on the virtual inertia concept for the dc MGs. Section III presents a multistage structure of dc MGs with CPLs and describes an accurate small-signal model of dc MGs. The stability analysis of the system and parameters range selection in the presence of the proposed controller are described in the Section IV. Simulation studies are presented in Section V. Finally, some conclusions are given in final section.

II. Proposed Virtual Inertia Control for DC MGs

In traditional power grids, the inertia indicates the ability of the system to prevent high frequency changes through injecting kinetic energy of rotating part in the occurrence of a fault. In this condition, the control system of synchronous generator (SG) will have enough time to compensate the active power. In SGs, the swing equation is a relationship that correlates input mechanical power, output electrical power, and the frequency. The imbalance equation, and the kinetic energy stored in the two poles of SG is given as [16]:

$$P_{set} - P_o - D_p(\omega - \omega_n) = J\omega\frac{d\omega}{dt} \quad (1)$$

where P_{set}, P_o, D_p, ω, ω_n and J are the reference active power, the output electrical power, the damping coefficient, the angular frequency, the nominal angular frequency, and the amount of inertia, respectively. When J and D_p increase (decrease), the rate of change of frequency (RoCoF) and frequency deviation are decreased (increased), respectively. In MGs, however, the damping coefficient, D_p, is a small value while the total inertia, J, changes mainly depending on the number of distributed generations (DGs) in the system [2]. For dc MGs, the amount of inertia is in fact the ability of the system to prevent high variation of the dc bus voltage due to turbulences. In order to study the virtual inertia concept, a simplified dc MG is shown in Fig. 2(a). By imitating relation (1), the balance current equation in the node connected to the dc load bus capacitor shown in Fig. 2(a) is obtained as follows:

$$i_{o2} - i_{in1} = C\frac{dv_{C2}}{dt} \quad (2)$$

where i_{o2}, i_{in1}, v_{C2}, and C are the injected current into the dc load bus from the source-side converter, the load current, the dc load bus voltage, and the dc load bus capacitor, respectively. Comparing (1) with (2) one can write that the dc link capacitor in a dc MG shows similar behavior as inertia in ac systems. When turbulence occurs in the load current, the dc link capacitor with rapid active power injection prevents the big changes in the dc link voltage. Thus, to increase the inertia in

dc MGs, size of the dc link capacitor has to be increased. Accordingly, instead of increasing capacity of the dc link capacitor physically, its size can be increased virtually using a virtual capacitor created by a control loop.

Assume that the variables in (2) are written as the sum of steady-state variables and their small perturbations the corresponding small-signal equation can be expressed as follows

$$\Delta i_{o2} - \Delta i_{in1} = C \frac{d\Delta v_{C2}}{dt} \tag{3}$$

In such a case, the amount of injected current can be obtained as

$$\Delta i_{o2}^{*} = -\left(C_v \frac{d\Delta v_{C2}}{dt} + \frac{1}{R_c} \Delta v_{C2} \right) \tag{4}$$

$$i_{o2}^{*} - I_{o2} = -C_v \frac{d\Delta v_{C2}}{dt} - \frac{1}{R_c} \Delta v_{C2} \tag{5}$$

where i^{*}_{o2}, I_{o2}, C_v and $1/R_c$ are the output current reference, the nominal output current, the virtual capacitor and the virtual-conductance analogous to the damping factor D_p of SGs, respectively. The negative sign in (4) shows negative feedback. By substituting (4) into (3), we obtain

$$-\Delta i_{in1} = (C + C_v) \frac{d\Delta v_{C2}}{dt} + \left(\frac{1}{R_c} \right) \Delta v_{C2} \tag{6}$$

According to (6), increasing the virtual inertia and the virtual damping factor will result in decreasing the rate of change of voltage (RoCoV) and dc voltage deviation.

General scheme of the proposed virtual inertia loop is illustrated in Fig. 2(b), where it is implemented in the primary control level providing reference for the inner current loop. The inner control loop mechanism applied to the system consists of two modules: voltage controller and current controller with their designed set points. The droop control is widely used to reach proper load power sharing in dc MGs. The voltage and current controllers employ conventional proportional-integral controllers due to zero steady state error and easy adjustment. However, the pure differentiator of the virtual capacitance in the proposed method may bring undesired high frequency noises to the system. For avoiding this issue, a first-order low-pass filter (LPF) is constructed in series with the virtual capacitance feedback. Meanwhile, the PWM delay is expressed as a first-order transfer function that depends on the sampling time. The proposed control approach can easily be implemented to all types of dc-dc converters. Here, without loss of generality, a multi-level structure of dc MGs interfaced with bidirectional buck converter is utilized.

III. Small-Signal Modeling of dc MGs with CPLs

A. Structure of dc MGs

A typical structure of a dc MG is shown in Fig. 1 [23], [27], [33]. In this structure, two types of energy sources i.e., PV and battery are considered. The dc MG shown in Fig. 1 has a three-level configuration. In the first level, namely the source stage, in order to absorb the maximum available power, the interfacing converter is employed for PV. Meanwhile, the interfaced converter for battery is used to generate constant output voltage. The second level is consist of interfacing bidirectional converter which establishes the local output bus. Finally, the third level is a common load bus. CPLs are connected to the common load bus in this stage. Different voltage levels can be used in dc MGs [33]. The PV with rated output voltage of 55 V and battery with rated output voltage of 48 V are selected in the first stage, and the output voltage, i.e., the source bus voltage is fixed at 200 V. In the meantime, the output voltage of the second stage is selected as 100 V.

Due to the nominal voltage of each bus, different types of interface converters are selected. For PVs in the first stage, unidirectional boost converter is used as the interface. For battery in the first stage, bidirectional boost converter is selected to achieve both of the charging and discharging operations. For the interfacing converter in the second stage, bidirectional buck converter is selected. For CPL that connected at the common load bus, unidirectional buck converter is utilized. In order to study the performance of the proposed virtual inertia-based controller, a general model of the dc MG with CPLs must be derived.

B. Small-Signal Model of dc MGs with CPLs

In order to investigate the effectiveness of the proposed virtual inertia function, a precise and model of the aforementioned dc MG needs to be considered. As mentioned, different types of converters are used in each level. Here, without loss of generality, it is assumed that the source stage fixes its output voltage, and its dynamic is faster than the second stage consist of interfaced buck converter. Thus, dynamic of the first stage is not considered and the simplified dc MG scheme shown in Fig. 2(a) is studied. The detailed analysis of the system model is discussed below. Here, subtitle "1" is used for CPL unidirectional buck converter, and subtitle "2" is used for bidirectional buck converter between source bus and local load bus.

For the point-of-load (POL) converter, a unidirectional buck converter with a resistor as its load is selected as an example to represent the CPL. As suggested in [33], the closed-loop input impedance of the POL converter as follows

$$Z_{IN1}(s) = \frac{\hat{v}_{C2}}{\hat{i}_{o2}}\Big|_{\hat{v}_{Ci}^{*}(s)=0} = \frac{R_L C_1 L_1 s^3 + L_1 s^2 + R_L \left(1 + V_{C2} k_{p1}\right) s + R_L V_{C2} k_{i1}}{R_L C_1 D_1^2 s^2 + \left(D_1^2 - k_{p1} D_1^2 V_{C2}\right) s - k_{i1} D_1^2 V_{C2}} \tag{7}$$

where C_1, L_1, R_L, V_{C2}, D_1, k_{p1} and k_{i1} are the capacitance, the inductance, the resistance load, the steady-state dc load voltage, the steady-state duty cycle, the proportional and integral terms

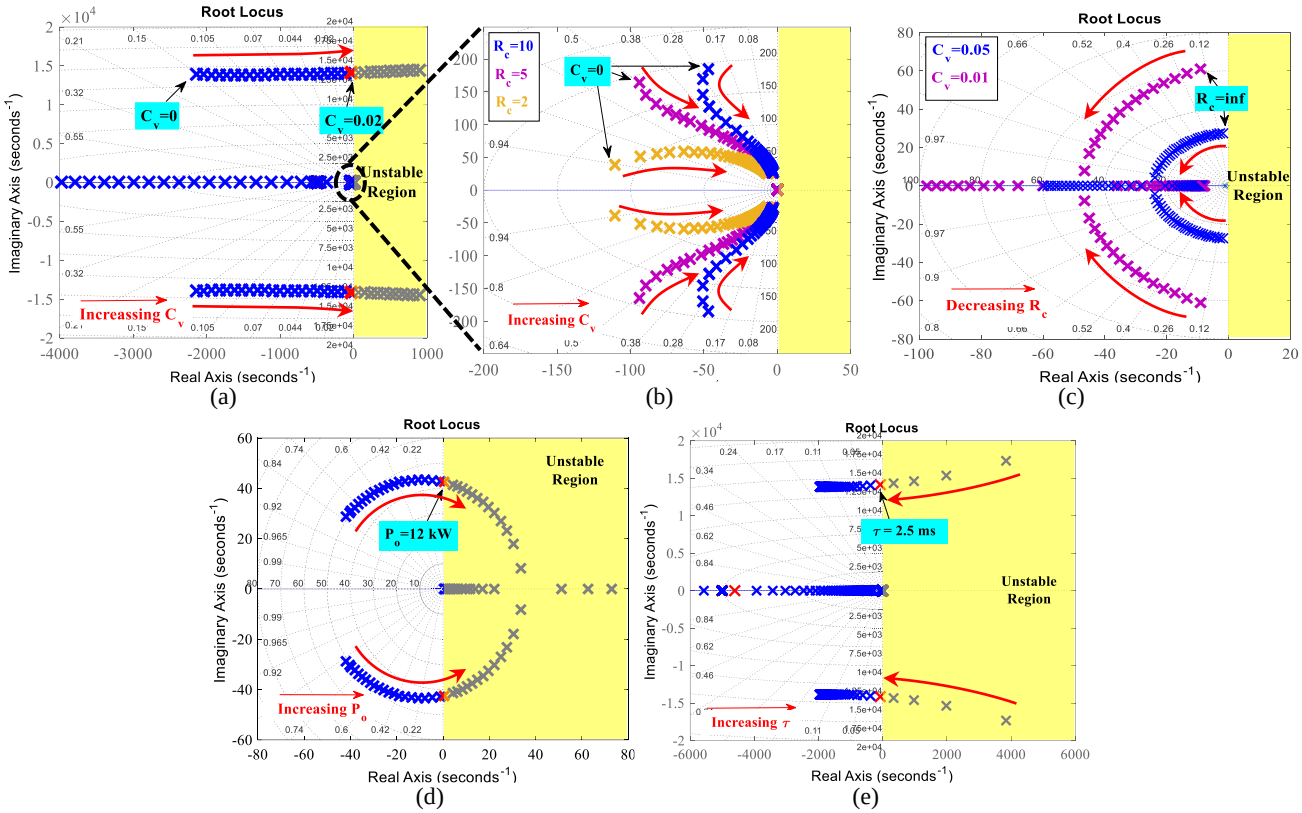


Fig.3. Trajectory of the system eigenvalues for the dc MG test system: (a) varying C_v, R_c and CPL=1kW, (b) a zoomed view of (a) in origin, (c) varying R_c while CPL=1 kW, (d) varying CPL while R_c=1 and C_v =0.01, (e) varying τ while R_c=5 and C_v =0.01 and CPL=1 kW.

of G_{pi1}. Equation (7) indicates a dynamic impedance that is more accurate comparing the pure negative resistance, i.e. $Z_{IN1}(s) = -R_1/D_1^2$.

For the bidirectional buck converters between the dc source (200 V) and dc local bus (100 V) if the switch turns on, it yields [34]

$$\begin{cases} L_2 \dfrac{di_{L2}}{dt} = v_{g2} - v_{C2} \\ C_2 \dfrac{dv_{C2}}{dt} = i_{L2} - i_{o2} \end{cases} \tag{8}$$

where v_{C2}, i_{L2}, and i_{o2} are the capacitor voltage, the inductor current and the output current, respectively. If the switch turns off, it yields

$$\begin{cases} L_2 \dfrac{di_{L2}}{dt} = -v_{C2} \\ C_2 \dfrac{dv_{C2}}{dt} = i_{L2} - i_{o2} \end{cases} \tag{9}$$

By applying averaging technique, the state-space equation is obtained as

$$\begin{cases} L_2 \dfrac{di_{L2}}{dt} = -v_{C2} + d_2 v_{g2} \\ C_2 \dfrac{dv_{C2}}{dt} = i_{L2} - i_{o2} \end{cases} \tag{10}$$

where d_2 is the duty cycle of the switch. From (10) and (7), the small-signal model is obtained as

$$\begin{bmatrix} \dfrac{d\hat{i}_{L2}}{dt} \\ \dfrac{d\hat{v}_{C2}}{dt} \end{bmatrix} = \begin{bmatrix} 0 & -\dfrac{1}{L_2} \\ \dfrac{1}{C_2} & -\dfrac{1}{Z_{IN1} C_2} \end{bmatrix} \begin{bmatrix} \hat{i}_{L2} \\ \hat{v}_{C2} \end{bmatrix} + \begin{bmatrix} \dfrac{D_2}{L_2} \\ 0 \end{bmatrix} \hat{v}_{g2} + \begin{bmatrix} \dfrac{V_{g2}}{L_2} \\ 0 \end{bmatrix} \hat{d}_2 + \begin{bmatrix} 0 \\ -\dfrac{1}{C_2} \end{bmatrix} \hat{i}_{o2} \tag{11}$$

where the steady-state values of variables represent with capital letter and the variables with "^" show the small-signal deviation. Let

$$A_2 = \begin{bmatrix} 0 & -1/L_2 \\ 1/C_2 & -1/Z_{IN1} C_2 \end{bmatrix}, B_{21} = \begin{bmatrix} D_2/L_2 \\ 0 \end{bmatrix}$$
$$B_{22} = \begin{bmatrix} V_{g2}/L_2 \\ 0 \end{bmatrix}, B_{23} = \begin{bmatrix} 0 \\ -1/C_2 \end{bmatrix}, C_{22} = [0 \quad 1]. \tag{12}$$

By taking the Laplace transform of (11) and combining the results, one can write that

$$\begin{aligned} \hat{v}_{C2}(s) = & \left[C_{22} (sI - A_2)^{-1} B_{21} \right] \hat{d}_2(s) \\ & + \left[C_{22} (sI - A_2)^{-1} B_{22} \right] \hat{v}_{g2}(s) \\ & + \left[C_{22} (sI - A_2)^{-1} B_{23} \right] \hat{i}_{o2}(s) \end{aligned} \tag{13}$$

In all dc-dc converters, the output voltage is a function of the control signal d, the turbulences caused by the voltage line of v_g and the load current of i_o. Therefore, the output voltage which equals to the capacitor voltage is obtained as a linear combination of these inputs as follows:

$$\hat{v}_{C2}(s)=G_{vd}\hat{d}_2(s)+G_{vg}\hat{v}_{g2}(s)-Z_{o2}\hat{i}_{o2}(s) \tag{14}$$

where

$$G_{vd}=\left[C_{22}\left(sI-A_2\right)^{-1}B_{21}\right],G_{vg}=\left[C_{22}\left(sI-A_2\right)^{-1}B_{22}\right]$$
$$Z_{o2}=-\left[C_{22}\left(sI-A_2\right)^{-1}B_{23}\right]. \tag{15}$$

By applying the proposed control method in Fig. 2(a), the small-signal model is achieved

$$\hat{d}_2(s)=\hat{v}^*_{C2}G_{pi2}G_{pi3}G_d-\hat{i}_{o2}G_{pi3}G_d\left[G_{pi2}R_d\right]-\hat{i}_{L2}G_{pi3}G_d$$
$$-\hat{v}_{C2}G_{pi3}G_d\left[\frac{G_{pi2}R_d}{Z_{IN1}}+G_{pi2}+G_{LPF}C_v s+\frac{1}{R_c}\right] \tag{16}$$

where, G_{LPF} = 1/(τs+1) and τ is the time constant of the LPF. Also, G_d = 1/(1.5T_{sPWM} s+1) represents the unit pulse width modulation delay and T_{sPWM} is the sampling period. The closed-loop transfer function between the output voltage and the reference voltage is as follows:

$$T_{21}=\frac{\hat{v}_{C2}(s)}{\hat{v}^*_{C2}(s)}=\frac{G_{pi2}G_{pi3}G_{vd}}{1+T(s)} \tag{17}$$

where

$$T(s)=$$
$$G_{vd}G_{pi3}G_d\left[Cs+\frac{1}{Z_{IN1}}+G_{LPF}C_v s+\frac{1}{R_c}+G_{pi2}\left(1+\frac{R_d}{Z_{IN1}}\right)\right] \tag{18}$$

Furthermore, the steady state value of the output voltage is obtained as follows:

$$v_{ss}=\frac{1}{1-R_d D_1^2/R_L}V^*_{C2} \tag{19}$$

The steady state value is only a function of the droop coefficient and load resistance. This value can improve the load division of several DG units into a dc MG by adjusting the steady state output voltage.

Finally, the relation between the output voltage of converter and the load current is obtained as

$$T_{22}=\frac{\hat{v}_{C2}(s)}{\hat{i}_{o2}(s)}=\frac{-Z_{o2}-G_{pi3}G_{vd}G_d\left(1+G_{pi2}R_d\right)}{1+T}. \tag{20}$$

IV. Stability Analysis and Parameter Selection

According to the precise small-signal model achieved in Section III-B, stability analysis can be studied by analyzing the eigenvalues of the transfer functions (17) and (20). The proposed controller parameters that affect stability are the virtual capacitor C_v, virtual resistance R_c and the low-pass filter time constant (τ). In order to obtain the system stable, the dominant poles of the small-signal model in (17) and (20) must be located in the left-half of the s-plane**.** The stability of the proposed controller with CPLs is investigated by varying the value of system parameters, as shown in Fig. 3. The trajectory of dominant poles with changing the virtual capacitance for various value of R_c and P_o=1kW is shown in Fig. 3(a). It can be seen that two poles move toward the unstable region. By selecting proper virtual capacitance, i.e., C_v < 0.02, the system stability is guaranteed. With increasing C_v, the dominant poles move toward the imaginary axis and the system behaves like a 2nd order system (see Fig. 3(b)). The trajectory of dominant poles when changing the virtual resistance and P_o=1kW is shown in Fig. 3(c). By increasing 1/R_c (decreasing R_c), the damping ratio of dominant poles increases and the response speed is decreased. Fig. 3(d) shows the unstable system trace when the CPL increases and C_v=0.01, R_c =1. It can be observed that increasing load power deteriorates the damping and causes instability. Fig. 3(e) shows the dominant poles of the system when the time constant of the LPF increases from 0 to 40 ms. It can be seen that two poles move toward the stable region. By selecting proper time constant, i.e., τ > 2.5 ms, the unstable poles move to the left side s-plane, hence the system stability is guaranteed.

V. Simulation Results

In order to validate the performance of the proposed control method, the dc MG test system (Fig. 1) is simulated in MATLAB/Simulink software. The parameters of the system are given in Table I.

A. Case I: Operation of dc MG with PV, Battery and CPL

For testing the proposed control strategy for the injection of virtual inertia, a typical dc MG including PV, battery and CPL is used. In order to track the maximum power from the PV system, a unidirectional boost converter is implemented between PV and dc MG. The bidirectional boost converter for the battery is employed to construct the local source bus with a voltage and current control loops. The source bus voltage is regulated at 200 V. By employing the bidirectional buck converter for interface converter, the load bus of the distributed generation unit is constructed. The load bus is regulated at the rated value of 100 V. The existence of the CPLs in dc MGs is the worst-case scenario from the stability perspective. Therefore, it is assumed that a CPL with power rate of 1kW is connected to the load bus. The PV output power, battery output power and CPL power are shown in Fig. 4, when the PV output power reference changes. In this case unit 1 only feeds the load. PV output power follows its reference value and with battery feed load power. When the output power of PV is more than the load power, the difference in their power is stored in battery (0.5 s < t < 0.6 s). Fig. 5 illustrates the PV output voltage, source bus voltage and load bus voltage when the PV output power reference changes. It can be seen that the load bus voltage is lower than its reference value due to the droop mechanism.

TABLE I
SYSTEM PARAMETERS OF THE DC MG

System	Parameters	Values	Parameters	Values
PV	L_4	5mH	V_{g4}	55V
system	C_4	0.5mF	V_{C4}	200V
Battery	L_3	4mH	V_{g3}	48V
system	C_3	0.8mF	V_{C3}	200V
Interface	L_2	1mH	V_{g2}	200V
converter	C_2	1mF	V_{C2}	100V
Load	L_1	10mH	Load Power	1 kW
	C_1	0.1mF	V_{C1}	50V

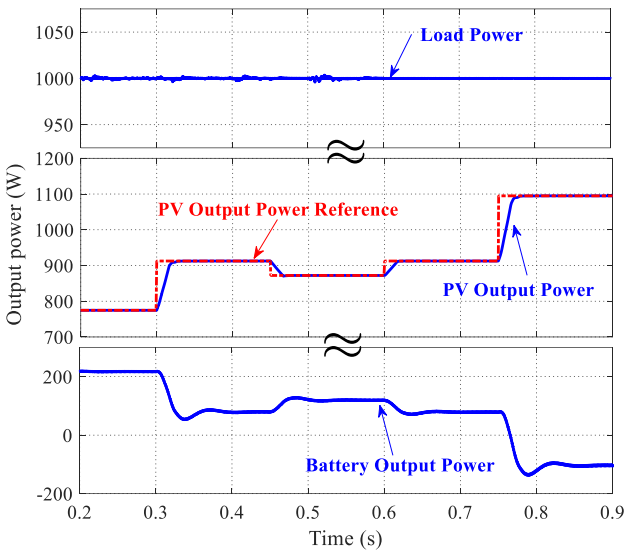


Fig. 4. Output power of different stage unit 1 when the PV output power reference changes.

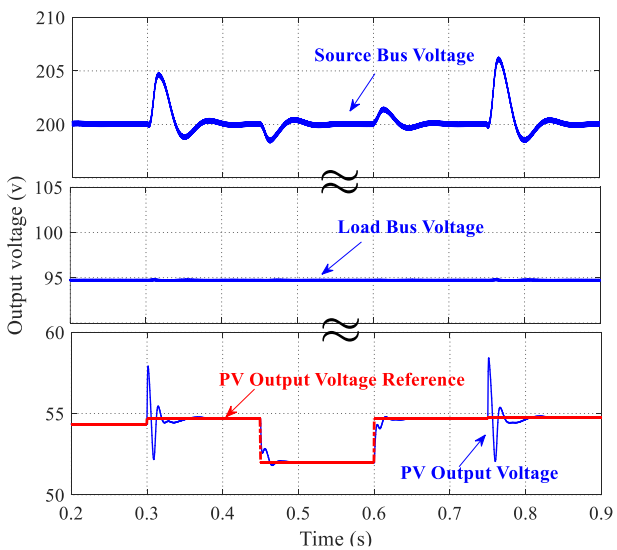


Fig. 5. Output voltage of different stage unit 1 when the PV output power reference changes.

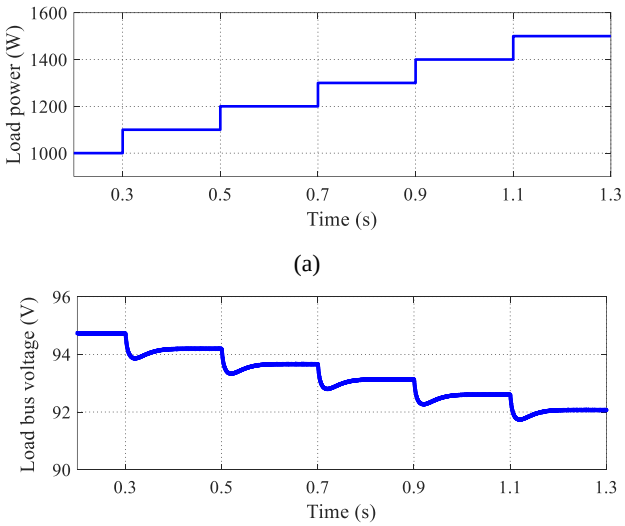


Fig. 6. Performance of the proposed VI solution under load power change: (a) load power step-up, (b) load bus voltage.

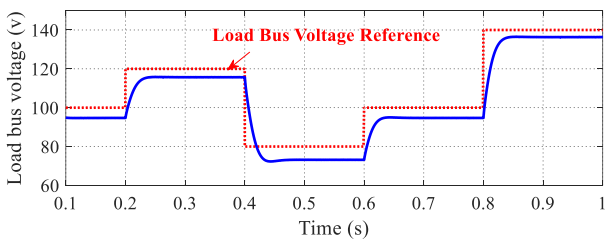


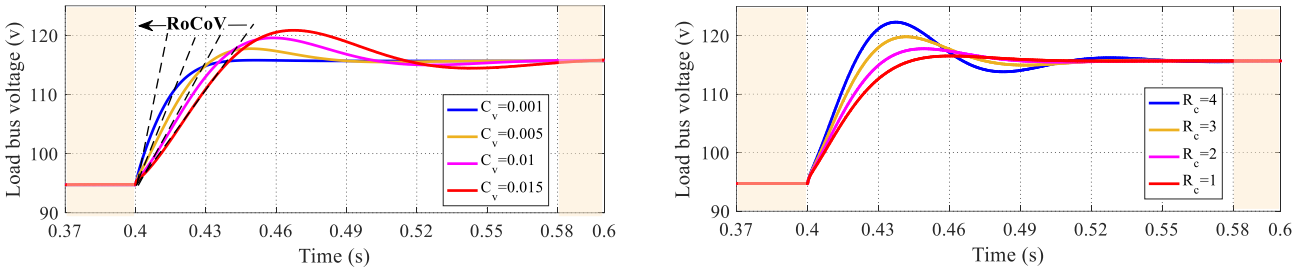
Fig. 7. Load bus voltage (blue solid line) following step changes in the voltage reference (red dashed line).

B. Case II: Varying of the Reference Voltage and Load Power

In this scenario, effectiveness of the proposed virtual inertia loop is studied under continuous load step-up change (see Fig. 6). During the test, the CPL varies from 1 to 1.5 kW by 0.1 kW load-step. As can be seen, by using the proposed virtual inertia, virtual damping and droop control, stable operation is guaranteed. In addition, the performance of the proposed controller under continuous voltage reference change is also studied. During the test, the reference voltage varies following the sequence of 100, 120, 80, 100, and 140 V. As it can be seen from Fig. 7, the stable operation is assured with the proposed VI.

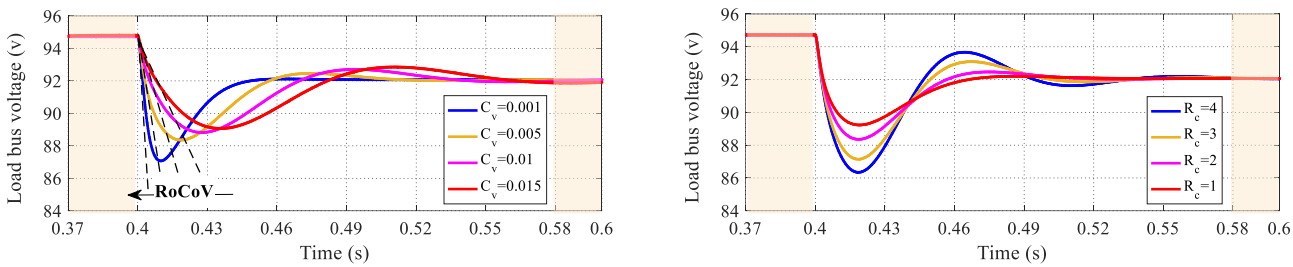
C. Case V: Impact of Virtual Parameters

Fig. 8 shows the dynamic response of dc load bus voltage for +20% change in voltage reference from V^*_{C2} = 100 V to V^*_{C2} = 120 V at t=0.4s. Dc bus voltage for various values of C_v while other system parameters are constant is shown in Fig. 8(a). As the C_v increases, the dc load bus voltage would smoothly change and the RoCoV decreases. This means that



(a) (b)

Fig. 8. Dynamic responses of dc load bus voltage after a step change in voltage reference: (a) varying C_v for R_c=2 and CPL=1kW, (b) varying R_c for C_v =0.005 and CPL=1 kW.



(a) (b)

Fig. 9. Dynamic responses of dc load bus voltage after a step change in load power: (a) varying C_v for R_c=2 and CPL=1kW, (b) varying R_c for C_v =0.005 and CPL=1 kW.

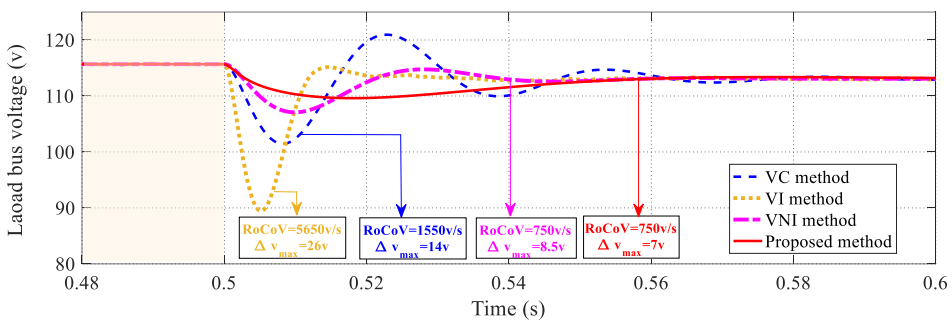


Fig. 10. Behavior of the dc bus voltage during a sudden load increase.

the inertia of the dc MG is increased. Thereby, the value of C_v denotes the synthetic inertia of the dc MG. However, by increasing C_v the system damping decreases and is prone to cause the DC bus voltage oscillation. This issue can be diminished by increasing damping coefficient ($1/R_c$) that effectively eliminates the low-frequency voltage oscillations. Fig. 8(b) shows dc bus voltage for various values of R_c while other system parameters are constant. By decreasing R_c (increasing $1/R_c$), the deviation of dc bus output voltage decreases. One can observe that virtual conductance $1/R_c$ can reduce the deviations of the dc bus output voltage and no influence on the RoCoV when voltage reference changes. Although virtual inertia response is more effective, it increases the settling time of the dc bus voltage. Consequently, a compromization between the settling time and the voltage deviation is needed for selecting the inertia and damping coefficients. The effectiveness of the proposed inertia response is tested under load power variation. Fig. 9 shows the dc load bus voltage for +50% step-change in load power from the initial value of P_o = 1 kW, to the final value of P_o = 1.5 kW at t=0.4s. In Fig. 9 (similar to Fig. 8), when C_v and/or $1/R_c$ increase (decrease), the RoCoV and voltage deviation will decrease (increase), respectively. Meanwhile, the parameters of inertia response have no influence on the steady-state performance.

The proposed method can be compared to previous works with implementing virtual parameter. Fig. 10 shows the comparison simulation results between the virtual capacitance (VC) method presented in [16], the virtual impedance (VI) method presented in [33], the virtual negative inductance (VNI) method presented in [32], and the proposed method for the same system parameters, loading conditions, and a 50% step change of load power at t = 0.5s. To have a better comparison, the same settling time is considered in the

methods. It is shown that the proposed controller provides quite better transient response, smaller RoCoV, smaller undershoot and no overshoot in comparison with other control techniques.

VI. Conclusion

This paper presents a control strategy based on virtual inertia to enhance dynamic response and stability of dc MGs interfaced with CPLs. In the proposed method, the derivative feedback coefficient (C_v) mimics the virtual inertia of synchronous machines, while the proportional feedback gains $1/R_c$ and R_d mimics the damping factor of synchronous machines and the conventional droop mechanism, respectively. A multistage dc MG with interface buck converter is considered to verify the effectiveness of the proposed control method. Comprehensive small-signal model of source-side buck converter and load-side buck converter are derived, and parameters selection are discussed based on root-locus analysis. The simulation results indicate that the proportional-derivative control can provide damping and inertia properties. When virtual capacitance and virtual damping coefficient increase (decrease), the RoCoV and the dc voltage deviation are decreased (increased).

References

[1] H. Bevrani, B. Francois, T. Ise, *Microgrid Dynamics and Control*, NJ, USA: Wiley, July 2017.

[2] H. Bevrani, M. Watanabe, Y. Mitani, *Power System Monitoring and Control*. Hoboken, NJ, USA: IEEE-Wiley, Jun. 2014.

[3] U. Tamrakar, D. Shrestha, M. Maharjan, B. P. Bhattarai, T. M. Hansen, R. Tonkoski, "Virtual inertia: Current trends and future directions," *Appl. Sci*., vol. 7, no. 7, pp. 654, Jun. 2017.

[4] S. Wei, Y. Zhou, and Y. Huang, "Synchronous Motor-Generator Pair to Enhance Small Signal and Transient Stability of Power System with High Penetration of Renewable Energy," *IEEE Access*, vol. 5, pp. 11505-11512, Jun. 2017.

[5] N. Soni, S. Doolla, M. C. Chandorkar, "Improvement of transient response in microgrids using virtual inertia," *IEEE Trans. Power Del.*, vol. 28, no. 3, pp. 1830-1838 Jul. 2013.

[6] E. Rakhshani, P. Rodriguez, "Inertia emulation in ac/dc interconnected power systems using derivative technique considering frequency measurement effects," *IEEE Trans. Power Syst*., vol. 32, no. 5, pp. 3338–3351, Sep. 2017.

[7] H. Bevrani, T. Ise, Y. Miura, "Virtual synchronous generators: A survey and new perspectives," *Int. J. Elect. Power Energy Syst.*, vol. 54, pp. 244-254, Jan. 2014.

[8] M. Ebrahimi, SA. Khajehoddin, MK. Ghartemani, "An improved damping method for virtual synchronous machines," *IEEE Trans. Sustainable Energy*, vol. 10, no. 3, pp. 1491-1500, Jul. 2019.

[9] A. Karimipouya, S. Karimi, H. Abdi, "Microgrid frequency control using the virtual inertia and ANFIS-based controller," *International Journal of Industrial Electronics, Control and Optimization*, vol. 2, no. 2, pp. 145-154, Apr. 2019.

[10] M. Guan, W. Pan, J. Zhang, Q. Hao, J. Cheng, X. Zheng, "Synchronous generator emulation control strategy for voltage source converter (VSC) stations," *IEEE Trans. Power Syst.*, vol. 30, no. 6, pp. 3093-3101, Nov. 2015.

[11] C. Li, J. Xu, C. Zhao, "A coherency-based equivalence method for MMC inverters using virtual synchronous generator control," *IEEE Trans. Power Del.*, vol. 31, no. 3, pp. 1369-1378, Jun. 2016.

[12] X. Meng, J. Liu, Z. Liu, "A generalized droop control for grid-supporting inverter based on comparison between traditional droop control and virtual synchronous generator control," *IEEE Trans. Power Electron*., pp. 1-1, Sep. 2018.

[13] Y.P. Kumar, R. Bhimasingu, "Fuzzy logic based adaptive virtual inertia in droop control operation of the microgrid for improved transient response," *Asia-Pacific Power and Energy Engineering Conf. (APPEEC)*, 2017, pp. 1-6.

[14] A. Karimi, Y. Jafarian, H. Bevrani, R. Mirzaei, "Frequency response improvement in microgrids: a fuzzy–based virtual synchronous generator approach," *International Journal of Industrial Electronics, Control and Optimization*, vol. 3, no. 2, pp.147-158, Apr. 2020.

[15] A. Fathi, Q. Shafiee, H. Bevrani, "Robust frequency control of microgrids using an extended virtual synchronous generator," *IEEE Trans. Power Syst.*, vol. 33, no. 6, pp. 6289-6297, Nov. 2018.

[16] W. Wu, Y. Chen, A. Luo, L. Zhou, X. Zhou, L. Yang, Y. Dong, J. M. Guerrero, "A virtual inertia control strategy for dc microgrids analogized with virtual synchronous machines," *IEEE Trans. Ind. Electron.*, vol. 64, no. 7, pp. 6005–6016, Jul. 2017.

[17] Z. Yi, X. Zhao, D. Shi, J. Duan, Y. Xiang, Z. Wang, "Accurate power sharing and synthetic inertia control for dc building microgrids with guaranteed performance," *IEEE Access*, vol. 7, no. 7, pp. 63698-708, May. 2019.

[18] W. Im, C. Wang, W. Liu, L. Liu, J. Kim, "Distributed virtual inertia based control of mutiple photovoltaic systems in autonomous microgrid," *IEEE/CAA J.Autom. Sinica*, vol. 4, no. 3, pp. 512-519, Jul. 2017.

[19] J. B. Zhu, C. D. Booth, G. P. Adam, A. J. Roscoe, C. G. Bright, "Inertia emulation control strategy for VSC-HVDC transmission systems," *IEEE Tran. Power Syst.*, vol. 28, no. 2, pp. 1277-1287, May. 2013.

[20] A. Hosseinipour, H. Hojabri, "Virtual inertia control of PV systems for dynamic performance and damping enhancement of dc microgrids with constant power loads," *IET Renew. Power Gener*., vol.12, no.4, pp.430-438, 2017.

[21] S. Samanta, J. P. Mishra, B. K. Roy, "Virtual dc machine: an inertia emulation and control technique for a bidirectional dc–dc converter in a dc microgrid," *IET Electr. Power Appl.*, vol. 12, no. 6, pp. 874-884, Mar. 2018.

[22] L. Herrera, W. Zhang, J. Wang, "Stability analysis and controller design of DC microgrids with constant power loads," *IEEE Trans. Smart Grid*, vol. 8, no. 2, pp. 881-888, Aug. 2015.

[23] M. Su, Z. Liu, Y. Sun, H. Han, X. Hou, "Stability analysis and stabilization methods of DC microgrid with multiple parallel-connected DC–DC converters loaded by CPLs," *IEEE Trans. Smart Grid*, vol. 9, no. 1, pp.132-142, Mar. 2016.

[24] M. Cespedes, X. Lei, S. Jian, "Constant-power load system stabilization by passive damping," *IEEE Trans. Power Electron.*, vol. 26, no. 7, pp. 1832-1836, Jul. 2011.

[25] J. Liu, W. Zhang, G. Rizzoni, "Robust stability analysis of DC microgrids with constant power loads," *IEEE Trans. Power Syst*., vol. 33, no. 1, pp. 851-860, Apr. 2017.

[26] S. Arora, P. Balsara, D. Bhatia, "Input–Output Linearization of a Boost Converter With Mixed Load (Constant Voltage Load and Constant Power Load)," *IEEE Trans. Power Electron*., vol. 34, no. 1, pp. 815-825, Jan. 2019.
[27] Q. Xu,C. Zhang, C. Wen, P. Wang, "A novel composite nonlinear controller for stabilization of constant power load in DC microgrid," *IEEE Trans. Smart Grid*, vol. 10, no. 1, pp. 752-761, Sep. 2017.
[28] M. Su, Z. Liu, Y. Sun, H. Han, X. Hou, "Stability analysis and stabilization methods of dc microgrid with multiple parallel-connected dc-dc converters loaded by CPLs," *IEEE Trans. Smart Grid*, vol.9, no.1, pp.132-142, 2018.
[29] K. A. Potty, E. Bauer, H. Li, J. Wang, "Smart resistor: stabilization of dc microgrids containing constant power loads using high-bandwidth power converters and energy storage," *IEEE Trans. Power Electron.*, vol. 35, no. 1, pp.957-967, Jan. 2020.
[30] M. Wu, D. D. C. Lu, "a novel stabilization method of LC input filter with constant power loads without load performance compromise in dc microgrids," *IEEE Trans. Ind. Electron*., vol. 62, no. 7, pp. 4552-4562, July 2015.
[31] M. N. Hussain, R. Mishra, V. Agarwal, "A frequency-dependent virtual impedance for voltage-regulating converters feeding constant power loads in a dc microgrid", *IEEE Trans. Ind. Appl.*, vol. 54, no. 6, pp. 5630-5639, Nov./Dec. 2018.
[32] S. Liu, P. Su, L. Zhang, "A virtual negative inductor stabilizing strategy for dc microgrid with constant power loads," *IEEE Access*, vol. 6, pp. 59728-59741, 2018.
[33] X. Lu, K. Sun, J.M. Guerrero, J.C. Vasquez, L. Huang, J. Wang, "Stability enhancement based on virtual impedance for dc microgrids with constant power loads," *IEEE Trans. Smart Grid*, vol. *6*, no. 6, pp. 2770-2783, Jun. 2015.
[34] R. W. Erickson, D. Maksimovic, *Fundamentals of power electronics.* Springer Science & Business Media, 2007.



Mehran Jami was born in Marivan, Iran (1986). He received the B.Sc. degree from University of Tehran, Tehran, Iran, and the M.Sc. degree from Tarbiat Modares University (TMU), Tehran, Iran, both in Electrical Engineering in 2012 and 2014, respectively. He is now working toward the Ph.D. degree in the control of power systems at the University of Kurdistan, Iran. He is currently a member of the Smart/Micro Grids Research Center (SMGRC) at the University of Kurdistan, Sanandaj, Iran. His research interests include modeling, analysis, design, and control of power electronic devices.



Qobad Shafiee (S'13–M'15–SM'17) received PhD degree in electrical engineering from the Department of Energy Technology, Aalborg University (Denmark) in 2014. He is currently an Assistant Professor, Associate Director of International Relations, and the Program Co-Leader of the Smart/Micro Grids Research Center at the University of Kurdistan, Sanandaj, Iran, where he was a lecturer from 2007 to 2011. His current research interests include modeling, energy management, control of power electronics-based systems and microgrids, and model predictive and optimal control of modern power systems.



Hassan Bevrani (S'90 - M'04 - SM'08) received PhD degree in electrical engineering from Osaka University (Japan) in 2004. Currently, he is a full professor and the Program Leader of Smart/Micro Grids Research Center (SMGRC) at the University of Kurdistan (UOK). From 2016 to 2019 he was the UOK vice-chancellor for research and technology. His current research interests include smart grid operation and control, power systems stability and optimization, Microgrid dynamics and control, and Intelligent/robust control applications in power electric industry.